IEEE Access
Multidisciplinary | Rapid Review | Open Access Journal

Received June 19, 2021, accepted June 29, 2021, date of publication July 12, 2021, date of current version July 22, 2021.

Digital Object Identifier 10.1109/ACCESS.2021.3096660

Efficiency Analysis of a Truncated Flip-FBMC in Burst Optical Transmission

MOHAMMED S. BAHAAELDEN[1], BEATRIZ ORTEGA[1], (Member, IEEE), RAFAEL PÉREZ-JIMÉNEZ[2], AND MARKKU RENFORS[3], (Life Fellow, IEEE)

[1]Instituto de Telecomunicaciones y Aplicaciones Multimedia (iTEAM), Universitat Politècnica de València, 46022 Valencia, Spain
[2]Institute for Technological Development and Innovation in Communications (IDeTIC), University of Las Palmas de Gran Canaria, 35001 Las Palmas de Gran Canaria, Spain
[3]Department of Electronics and Communications Engineering, Tampere University of Technology, 33720 Tampere, Finland

Corresponding author: Mohammed S. Bahaaelden (moba2@doctor.upv.es)

This work was supported in part by the Research Agency under Project RTI2018-101658-B-I00 and Project TEC2017-84065-C3-1-R, in part by the European Cooperation in Science and Technology COST Action "European Network on Future Generation Optical Wireless Communication Technologies (NEWFOCUS)" under Grant CA19111, and in part by Generalitat Valenciana under Grant PROMETEO 2017/103.

ABSTRACT A novel Flip-filter bank multicarrier (Flip-FBMC)-based transmultiplexer (TMUX) with offset quadrature amplitude modulation is proposed to enhance the transmission performance compared to a conventional Flip-OFDM system. Moreover, the possibility to reduce the TMUX response (latency) and increase spectral efficiency is investigated for the first time through a tail shortening method. The proposed design is based on a biorthogonal form for visible light communication (VLC) to increase the flexibility of design requirements. However, spectral efficiency suffers from the ramp-up and the ramp-down at the beginning and end, respectively, of a data burst. Hence, as a penalty, Flip-FBMC imposes 9 more symbols than a Flip-OFDM packet and two factors compared to a DCO-FBMC burst. Hard truncation of the lowest energy tail minimizes latency and limits the system penalty to 2.5 symbols, which is lower than that of DCO-FBCM by 2 symbols. The results show that the prototype filter of the Heisenberg factor ($\approx$1) is highly effective in reducing the energy loss of truncated tails and reduces the symbol error rate (SER). The Flip-FBMC gain over a direct line-of-sight VLC channel is analyzed, and the channel estimation of a truncated burst, which is based on the interference approximation method (IAM) of IAM-C type, exhibits a superior performance of 1.5 dB at 10^{-3} SER over the IAM-R method and 1 dB at 10^{-5} SNR over a cyclic prefix of 1 point Flip-OFDM. On the other hand, the analysis reveals that IAM-C is slightly impacted by the truncated burst compared to the nontruncated version.

INDEX TERMS Filter bank multicarrier (FBMC), hard truncation methods, Heisenberg factor, interference approximation method, visible light communication (VLC), Flip-OFDM.

I. INTRODUCTION

In the recent years, visible light communication (VLC) has attracted considerable attention due to its immunity to electro-magnetic interference, its freedom from health hazards, and its unlicensed spectrum. It is rapidly emerging as a compelling technology for supplementing conventional radiofrequency (RF) communications [1].

The most widespread modulation techniques in VLC based on a unipolar real-time signal are DC-offset orthogonal frequency division multiplexing (DCO-OFDM), asymmetric clipped optical OFDM (ACO-OFDM) and Flip-OFDM [2], [3]. The DCO-OFDM scheme requires a DC bias voltage to transform a bipolar-real optical signal into unipolar form to be employed in intensity modulation and direct detection (IM/DD) communication systems at the expense of a high peak-to-average power ratio (PAPR), especially for large constellation signals. The performance of DCO-OFDM depends on the bias level that relays on the constellation sizes [4]. Furthermore, the excessive biasing leads to inefficient optical power, whereas the use of a low DC bias value results in significant spectral spreading and enormous inter-carrier interference (ICI).

The associate editor coordinating the review of this manuscript and approving it for publication was Filbert Juwono.

Flip-OFDM has a superior performance over the well-known DCO-OFDM scheme at the expense of a 50% bandwidth penalty [5]. Moreover, Flip-OFDM shows an identical error performance to the ACO-OFDM technique but with 50% less receiver hardware complexity [6]. As is well known, OFDM subcarrier bands exhibit large sidelobes, which, under interference, may lose their orthogonality, and the power leakage of one sidelobe can be high enough to disable several neighboring channels. Additionally, the insertion of cyclic prefixes (CPs) into

OFDM to eliminate the intersymbol interference (ISI) of rectangular pulses, which are very sensitive to synchronization errors, drives reductions in both spectral and power efficiency [7], [8].

OFDM with offset quadrature amplitude modulation (OFDM/OQAM), also known as filter bank-based multicarrier (FBMC) modulation, has been considered an attractive alternative to traditional OFDM because of its ability to reduce the out-of-band power leakage, boost the gain in spectral efficiency, and overcome the limitations arising from synchronization errors.

Furthermore, OFDM/OQAM has been adopted and modified as DC offset FBMC (DCO-FBMC) for VLC in [9], where the information rate was increased by 9% because of the elimination of the 16-CP symbols overhead and the guard bands. Despite the influence of intrinsic imaginary interference (IMI), which is considered the major obstacle in the FBMC mechanism, the error performance was found to be identical to that of DCO-OFDM by using an isotropic orthogonal transformation algorithm (IOTA) filter with a channel estimation (CE) based on the interference approximation method (IAM) of IAM-R type.

However, the CE-based IAM-C type was assessed as the optimum choice for signal estimation (2 dB better performance over OFDM in an RF field [10]) inasmuch as its pseudo-pilots have a larger magnitude than IAM-R and a lower PAPR compared to other CE-based preambles (i.e., the extended IAM-C, IAM-R and other interference cancellation methods) [11], [12]. From such a perspective, the preamble has been introduced in coherent optical communications [13], [14].

DCO-FBMC has also exhibited a superior bit error rate over the traditional technique by using a Mirabbasi-Martin filter and pilot-aided CE to combat IMI [15], while DCO-OFDM requires a CP of one sample to combat ISI over a 20 cm line-of-sight (LOS) free space distance using a laser diode at 642 nm.

However, FBMC/OQAM signals exhibit a penalty in terms of the number of symbols to transmit due to the transitions of the redundancy tails at both sides of a data burst, which leads to a reduction in their spectral efficiency and therefore a significant throughput reduction, especially in short-packet transmission. In the RF domain, several methods have been proposed to increase spectral efficiency, such as a hard truncation method [16], which degrades the system performance using a PHYDYAS filter (a Martin filter with overlapping factor $K = 4$). For a given application, the performance of a prototype filter is evaluated through some of its figures of merit, such as the Heisenberg parameter (ξ), which is a measure of how well a localized pulse deals with such a harsh environment [17], [18].

In this work, for the first time to the authors' knowledge, we propose a novel Flip-FBMC scheme-based transmultiplexer (TMUX) model in [19] as a good alternative to the traditional Flip-OFDM technique in [3]. Our scheme is based on a biorthogonal form to increase the flexibility of the design requirements. Furthermore, a modified method of hard redundancy tail truncation is investigated to be employed in a VLC system for the first time to increase its information rate and reduce its reconstructed delay (TMUX response) at the AFB output. Moreover, the truncation impact is evaluated according to the quality of the retrieved signal. An analysis comparison between IOTA and Martin filters based on their Heisenberg factor leads to the selection of the optimum one over the proposed shortened tails and different modulation orders. In Flip-FBMC, the two variants of the IAM methods in [11] are employed to mitigate the influence of IMI and enhance the accuracy of CE over the conventional Flip-OFDM technique. In addition, the performance of the truncated system with IAM-R and IAM-C preambles is reported with respect to the nontruncated version.

The remainder of this paper is structured as follows. In section II, we introduce a biorthogonal Flip-FBMC modulation format for an IM/DD LOS optical system. Section III presents the performance results and a comparison with Flip-OFDM. Section IV presents a tail shortening method to further improve spectral efficiency and the TMUX-response. Section V presents the estimation of indoor LOS channel state information by using a one-tap zero forcing equalizer (ZF) with IAM-R and IAM-C channel estimation methods, both based on truncated burst transmission. Finally, the concluding remarks are provided in section VI.

II. FLIP FBMC-TMUX SYSTEM DESCRIPTION

FBMC-TMUX is considered a biorthogonal system with sufficient flexibility in its design requirements since either the inverse fast Fourier transform (IFFT) or the fast Fourier transform (FFT) can be employed at the receiver (RX) side [20], [21], where both designs share the same performance results. The core of the FBMC system is its TMUX configuration with the fundamental processing blocks of OQAM pre-processing and a synthesis filter bank (SFB) that combines sub-band signals into one filtered signal. At the RX side, the analysis filter bank (AFB) includes matching receiver filters, and OQAM post-processing allows the retrieval of the complex input signal [22]–[26]. A schematic diagram of Flip-FBMC based on a biorthogonal form for a VLC system is depicted in Fig. 1, which shows the flexibility at the RX side, where either RX_1 or RX_2 is needed to retrieve the input signal. The bipolar-FBMC signal $X(k)$ at the transmitter (TX)

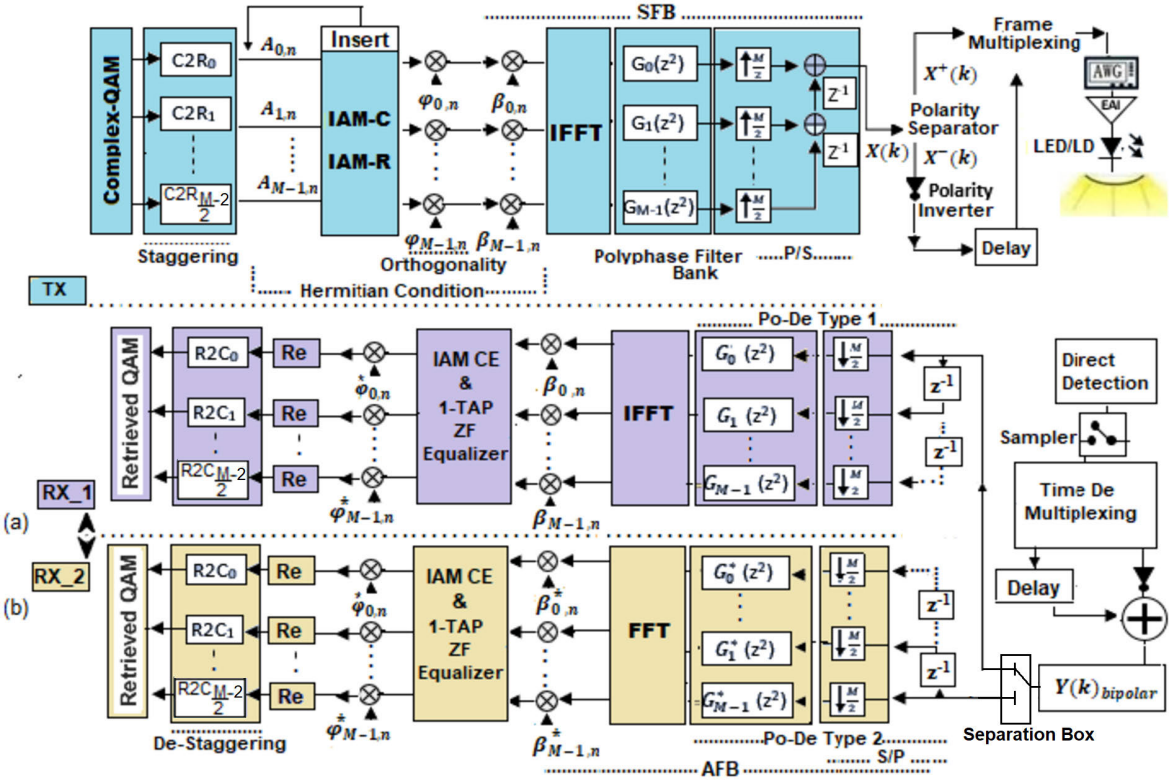

FIGURE 1. Polyphase implementation of the biorthogonal Flip-FBMC-based TMUX configuration in a VLC system to recover the input QAM signal by using either (a) an IFFT-based RX_1 or (b) an FFT-based RX_2.

side can be expressed as follows [21]:

$$X(k) = \sum_{n=0}^{N-1} \sum_{m=0}^{M-1} A_{m,n} P_{m,n}[k]$$

$$X(k) = \sum_{n=0}^{N-1} \sum_{m=0}^{M-1} A_{m,n} \varphi_{m,n} \underbrace{e^{-j\frac{2\pi}{M}m \cdot \frac{(M*K+1)-1}{2}}}_{\beta_m} * p\left[k - n\frac{M}{2}\right] e^{j2\pi \frac{mk}{M}} \quad (1)$$

with

$$\varphi_{m,n} = e^{j\frac{\pi}{2}(m+n)} = j^{(m+n)} \quad (2)$$

where M denotes the total number of subchannels ($2^*(M/2\text{-}1)+2$) in the filter bank due to the Hermitian symmetry provided in Table 1 and N is the total number of employed symbols. $P_{m,n}[k]$ describes the pulse shape of the prototype filter, and $A_{m,n}$ denotes two staggered pulse amplitude modulation (PAM) symbols. The phase shift term between adjacent PAMs is indicated by $\varphi_{m,n}$. The OQAM staggering block is calculated according to [24], [26] as:

$$A_{m,\,2n} = \begin{cases} \mathrm{Re}\left[C_{m,\,n}\right] & m \text{ even} \\ \mathrm{Im}\left[C_{m,\,n}\right], & m \text{ odd}, \end{cases} \quad (3)$$

and

$$A_{m,\,2n+1} = \begin{cases} \mathrm{Im}\left[C_{m,\,n}\right] & m \text{ even} \\ \mathrm{Re}\left[C_{m,\,n}\right], & m \text{ odd}, \end{cases} \quad (4)$$

The complex-to-real conversion block ($C2R_{m,n}$) converts the input symbol of a complex QAM ($C_{m,n}$) into real adjacent symbols with a $T/2$ relative time offset to carry the quadrature and in-phase information of the input-complex QAM. Hence, the staggering process results in upsampling by a factor of 2.

The real successive symbols $A_{m,n}$ are $\pi/2$ phase-shifted using $\varphi_{m,n}$ to preserve their orthogonality. To obtain a bipolar-real signal in the FBMC-TMUX transmitter side, the orthogonal-complex symbols with their corresponding phase-shift of β_m must satisfy Hermitian symmetry conditions, as presented in Table 1.

Assume that Hermitian symmetry is satisfied between the incoming signal and its transpose-conjugate feeding the IFFT processing block. Hence, a bipolar-real signal is processed convolutionally by a bank of M uniform-shifted replicas of a prototype filter, which are symmetric real-valued and delayed by $((M*K+1)\text{-}1)/2$ samples to provide the required causality. The $(M*K+1)$ term indicates a filter length with a K overlapping factor that controls the number of symbols that overlap in time domain. The biorthogonal system refers to the possibility of retrieving the transmitted signal either with an IFFT-based AFB at the first receiver (RX_1) by using type-1 polyphase decomposition (Po-De) as shown in Fig. 1(a) or with an FFT-based AFB by employing type-2 polyphase filters at the second receiver (RX_2) as shown in Fig. 1(b). The synthesis filters $g_m(k)$ represent the m^{th} shifted version of prototype filter $p[k]$ of L_p length at the transmitter side,

TABLE 1. Hermitian symmetry of the input signal in a Flip- FBMC-based TMUX structure.

Subcarrier Number \ Symbol Number	1	2	…	2N
1	0	0	0	0
2	Re (A (2,1)) β_2	J * Im (A (2,2)) β_2	⋯	$\varphi_{2,2N}$ * Im (A (2,2N)) β_2
3	J * Im (A (3,1)) β_3	-1 * Re (A (3,2)) β_3	⋯	……
4	-1 * Re (A (4,1)) β_4	-J * Im (A (4,2)) β_4	⋯	……
5	-J * Im (A (5,1)) β_5	Re (A (5,2)) β_5	⋯	……
……	……	……	…	……
M/2+1	0	0	0	0
……	……	……	…	……
M -1	(J * Im (A (3,1)) β_3)*	(-1 * Im (A (3,2)) β_3)*	⋯	……
M	(Re (A (2,1)) β_2)*	(J * Im (A (2,2)) β_2)*	⋯	($\varphi_{2,2N}$ * Im (A (2,2N)) β_2)*

while $f_m(k)$ is the m^{th} analysis filter at the receiver. Through type-2 Po-De, $f_m(k)$ represents a complex-conjugated and time-reversed model of a synthesis filter [18] as follows:

$$g_m(k) = p[k]e^{j2\pi \frac{mk}{M}} \frac{\overbrace{(M*K+1)}^{L_P}-1}{2}$$
$$f_m(k) = g^*\left[L_p - 1 - m\right] \tag{5}$$

It is worth mentioning that an IFFT-based AFB is very straightforward to implement, as no extra flipping is required as in a type-2 Po-De, but to emphasize the link and provide better backward compatibility to OFDM, the FBMC-TMUX is practical if deployed with an FFT-based AFB [21], [22].

The bipolar FBMC signal $X(k)$ is obtained by upsampling in a ratio of $M/2$ to compensate for the rate loss due to the $T/2$ relative time offset for OQAM mapping, followed by combining sub-band signals into one real filtered signal; this process is called parallel-to-serial conversion (p/s) [25]. The $X(k)$ signal mutates to a unipolar format as $X^+(k)$ and $X^-(k)$ utilizing flip processing techniques that are juxtaposed in consecutive FBMC subframes to be employed for IM of the LED, and that can be calculated according to [3], [6]:

$$X^+(k)_{\text{Positive\_part}} = \begin{cases} x(k) & \text{if } k \geq 0 \\ 0 & \text{otherwise} \end{cases}$$
$$X^-(k)_{\text{Flipped\_part}} = \begin{cases} x(k) & \text{if } k < 0 \\ 0 & \text{otherwise} \end{cases} \tag{6}$$

The successively received FBMC subframes $Y^+(k)$ and $Y^-(k)$ are subtracted to regenerate the bipolar form as:

$$Y(k)_{\text{FBMC\_bipolar}} = \underbrace{X^+(k) \otimes h^+(l) + Z^+(k)}_{Y^+(k)} - \underbrace{(X^-(k) \otimes -h^-(l) + Z^-(k))}_{Y^-(k)} \tag{7}$$

where $\otimes$ represents convolution, $h(l)$ is an optical channel impulse response with l taps, and Z represents noise samples of additive white Gaussian noise (AWGN). The n^{th} non-equalized received symbols of m^{th} subcarriers can be achieved by demodulating the received signal given in Eq. (7) as [9], [27]:

$$R_{m,n} = \sum_{k=-\infty}^{\infty} Y(k)P_{m,n}[k]^*$$
$$R_{m,n} = H_{m,n}A_{m,n} + j * \underbrace{\sum_{m0,n0 \in \Omega} H_{m0,n0}A_{m0,n0}\left\langle P_{m,n}[k], P_{m0,n0}[k]^*\right\rangle}_{\text{Intrinsic interference}} + \underbrace{\sum_{k=-\infty}^{\infty} Z(k)P_{m,n}[k]^*}_{z_{m,n}}$$
$$R_{m,n} = H_m A_{m,n} + H_m j A_{m,n}^{\text{intrinsic}} + Z_{m,n} \tag{8}$$

where H_m is the m^{th} channel frequency response at the frequency-time (FT) point (m,n), $Z_{m,n}$ denotes Gaussian noise, and $\boldsymbol{\Omega}$ indicates the set of FT points around (m,n). Extra attention is required at the TMUX-receiver side: the delay parameter $\Delta\delta$ arises to ensure causality, while the reconstructed delay (TMUX-latency) $\Delta\Upsilon$ is introduced at the evaluated symbols and can be written as:

$$\Delta\Upsilon = \frac{2}{IFFT_{\text{Size}}}\left(L_p - 1 + \Delta\delta\right) \tag{9}$$

These parameters depend on the filter length used, where a longer prototype drives to higher latency at the TMUX output [17], [22]. Interference can be generated as imaginary intrinsic interference (IMI) $jA_{m,n}^{\text{intrinsic}}$ through the m^{th} multi-path channel, which is inherent in FBMC mechanisms and cannot be prevented. On the other hand, real self-interference can be avoided by using a well-designed prototype filter [27], [28]. From (8), the intrinsic interference term is purely imaginary if the channel response is 1, and the received signal can be derived as:

$$A_{m,n}^{\text{Received}} = \text{Re}\left\{R_{m,n}\right\} \tag{10}$$

Then, the input complex QAM symbol can be retrieved using a real-to-complex conversion-block ($R2C_{m,n}$) as expressed in [26].

$$C_{m,n}^{\text{Retrieved}} = \begin{cases} A_{m,2n}^{\text{Received}} + jA_{m,2n+1}^{\text{Received}} & m \text{ even} \\ A_{m,2n+1}^{\text{Received}} + A_{m,2n}^{\text{Received}} & m \text{ odd}, \end{cases} \quad (11)$$

III. PERFORMANCE ANALYSIS OF A DIRECT LOS VLC CHANNEL

The performances of the novel Flip-FBMC-based TMUX and the conventional one in [6] are assessed in terms of the symbol error rate (SER), the spectral efficiency and the computational complexity over various overlapping factors of different employed filters. Through the simulation experimental setup of the LOS optical wireless link that is tabulated in Table 2, the channel DC gain of an LOS optical wireless link is considered and can be calculated as follows [29]:

$$h_{Los} = \begin{cases} \dfrac{(\mathrm{Q}+1)Ar}{2\pi d^2}\cos^{Q}(\theta)T_S(\Psi)g(\Psi)\cos(\Psi) \\ \quad 0 \le \Psi \le \Psi_C \\ 0, \quad \Psi > \Psi_C \end{cases} \quad (12)$$

where Ψ is the incident angle, Θ is the irradiance angle, Ar is the physical area of the photodiode (PD), and $g(\Psi)$ is the gain of the optical concentrator with a half-angle FOV (field of view) of Ψ_C, $T_S(\Psi)$ is the gain of the optical filter, and d represents the distance between the light-emitting diode (LED) and PD. The Q parameter describes the order of Lambertian emission with a semi-angle at half power $\phi_{(1/2)}$ and can calculated according to [29]–[31]:

$$Q = -\ln(2)/\ln\left(\cos\phi_{1/2}\right) \quad (13)$$

TABLE 2. Simulation system parameters.

Parameters	Value	
Utilized technique	Flip FBMC	Flip OFDM
Field of view (FOV)	60°	
Link distance	80 cm	
Gain of an optical filter	1.0	
Responsivity of PIN 1601FS-AC	0.2 A/W @ 450 nm	
Lens refractive index	1.5	
Transmitted power	4.5 mW	
Area of PD	0.125 mm^2	
AWGN	Shot & thermal noise	
IFFT size (M)	64 samples	
Constellation mapping	Low-high	
Prototype filter	Martin & IOTA	Rectangular
Overlapping factor (K)	3, 4 & 5	Non
Number of transmitted symbols	1-100	

The system SER is evaluated as a function of the electrical signal-to-noise ratio (SNR), as depicted in Fig. 2. In this work, the parameters employed to estimate the LOS channel

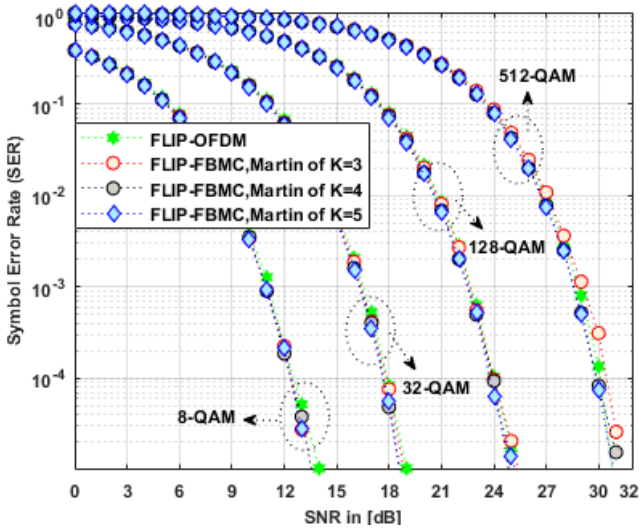

FIGURE 2. Performance comparison between the Flip-FBMC schemes of various overlapping factors and those over different M-QAM modulation formats in the VLC LOS channel.

gain are based on [30], where a blue μLED having a peak wavelength of 450 nm is used, and the influences of shot and thermal noise are modeled as AWGN. The simulation results in section III and IV are obtained assuming the optical channel state information in (12) is known at the receiver.

The most common choices of filter lengths are $IFFT_{Size}$*K, $IFFT_{Size}$*K-1, and $IFFT_{Size}$*K+1, where $IFFT_{Size}$ represents one block of M subcarriers (one symbol = 1 block of M samples). In addition, shorter or longer than those filter values cause a degradation in system performance. The proposed biorthogonal system is tested by using the Martin filter in [15] which has a length of $IFFT_{Size}$*K+1 because it represents the optimum length choice for the reconstruction quality [31]. To evaluate the performance comparison, each overlapping factor ($K = 3$, $K = 4$ and $K = 5$) of the proposed system is tested on a low to high constellation mapping.

It can be seen from Fig. 2 that the overlapping factor of 3 presents a higher SER performance than the conventional technique with an increasing constellation order, while the overlapping factor of 4 is shown to be the optimum choice due to a slightly improved error performance over Flip-OFDM. Even though $K = 5$ introduces an improvement almost identical to that of $K = 4$, the boost in computational complexity, filter latency, and gain reduction in spectral efficiency are the most significant drawbacks [22].

The information burst samples conveyed over the modulation bandwidth of the LED can be given by:

$$Flip - FBMC_{\text{burst}} = 2\left(IFFT_{\text{Size}}{}^{*}(N + K + 0.5)\right) \quad (14)$$

The length of the Flip-OFDM burst with no CPs or guard bands is only 2^* (N $IFFT_{Size}$) samples. Thus, Flip-OFDM exhibits a higher spectral efficiency than the proposed scheme. However, a superior gain in the spectral efficiency of an optical FBMC compared to an optical OFDM due to

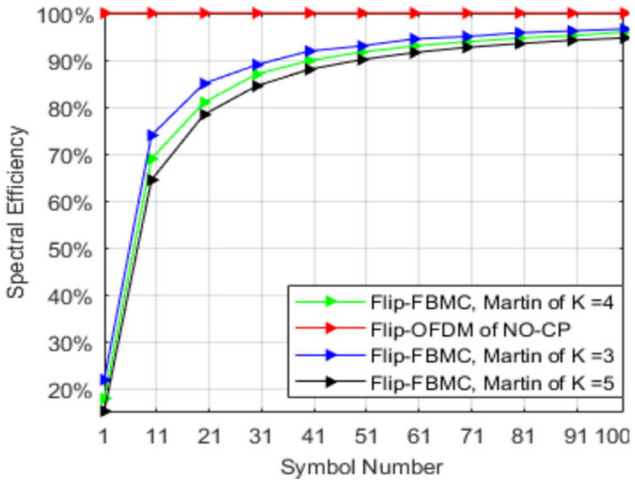

FIGURE 3. Spectral efficiency comparison at a flat-VLC channel.

the CPs and guard bands utilized in the OFDM structure to combat ISI has been reported [9].

Fig. 3 shows the spectral efficiency of Flip-OFDM with no CP and a Flip-FBMC using a Martin filter with different overlapping factors. It is observed that the spectral efficiency of the proposed approach is boosted with reduced K and increased frame duration, where a limited packet shows a significant drop in the information rate from the influence of redundancy tails at both sides of packet data transmission. Thus, a tail shortening process is an essential procedure to enhance the spectral efficiency, especially for short-packet transmission [32], as detailed in section IV.

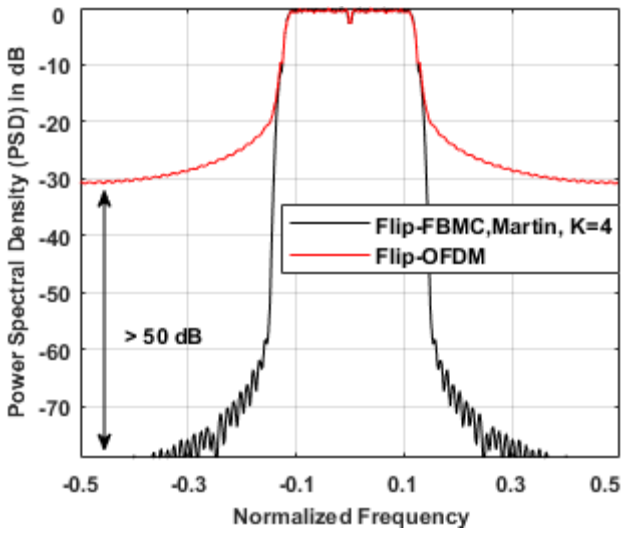

FIGURE 4. Power spectral density of Flip-FBMC vs Flip-OFDM.

The power spectral density (PSD) of the proposed scheme is examined through an evaluation of the out-of-band emission (OOBE) with respect to the classic system. The major feature of the FBMC is its low OOB radiation, which allows more efficient spectrum sharing between users [33]. Fig. 4 illustrates the capability of the considered Flip-FBMC technique to reject the Flip-OFDM energy leakage of up to 50 dB, which also contributes to minimizing synchronization errors.

The most significant drawback in the FBMC mechanism is its computational complexity [34]. However, regarding [35], FBMC-TMUX-based polyphase systems present less complexity than the one proposed in [15] due to the avoidance of unnecessary operations in frequency spreading. For the sake of comparison, the complexity of the multiplication (M_{com}) and addition (A_{com}) terms required to transmit one block of symbols for both techniques using an FFT Split-Radix algorithm is in [22], [35] and can be calculated as:

$$\begin{aligned} M_{\text{com}_{\text{Flip-FBMC}}} &= \underbrace{2}_{\text{OQAM}} * (\underbrace{2IFFT_{\text{Size}}}_{\beta} \\ &\quad + \underbrace{(IFFT_{\text{Size}} \left(\log_2 (IFFT_{\text{Size}}) - 3\right) + 4)}_{IFFT} + \underbrace{2L_P}_{SFB}) \end{aligned} \tag{15}$$

$$\begin{aligned} A_{\text{com}_{\text{Flip-FBMC}}} &= 2 \left(3IFFT_{\text{Size}} \left(\log_2 IFFT_{\text{Size}} - 1\right) + 4\right) \\ &\quad + 2IFFT_{\text{Size}} + 4 \left(L_P - IFFT_{\text{Size}}\right) \end{aligned} \tag{16}$$

$$\begin{aligned} M_{\text{com}_{\text{Flip-OFDM}}} &= \underbrace{IFFT_{\text{Size}} \left(\log_2 (IFFT_{\text{Size}} - 3) + 4\right)}_{IFFT} \end{aligned} \tag{17}$$

$$\begin{aligned} A_{\text{com}_{\text{Flip-OFDM}}} &= 3IFFT_{\text{Size}} \left(\log_2 IFFT_{\text{Size}}\right) - 3IFFT_{\text{Size}} + 4 \end{aligned} \tag{18}$$

As presented in the equations above, Flip-OFDM has much less hardware complexity than the proposed one because of an extra β term and M branch for each AFB and SFB for a given filter length. It can also be seen that the hardware complexity of Flip-FBMC is slightly reduced by using lower overlap factors. In addition, the short filter length of ($IFFT_{Size}$∗K-1) is preferable in terms of complexity since the influence of β can be neglected [22].

IV. TAIL SHORTENING THROUGH A HARD TRUNCATION TECHNIQUE

Further spectral analysis is required to optimize the bandwidth efficiency of the proposed system, and consequently, a short packet transmission is considered only to gain better insight into the impact of redundancy tails at both ends of the bipolar packet and the proposed shortening method, as depicted in Figs. 5, 7 and 8. By employing the Flip-FBMC scheme, the information burst samples expressed in (14) are bandwidth-limited because of the long filter impulse response, which imposes a ramp-up (initial transition) of 1.5 symbols, and a ramp-down (final transition) of 2.5 symbols at the beginning and end of the bipolar FBMC burst in addition to a required half-symbol of data packet transmission, which is required in the Flip-FBMC mechanism. These overhead blocks, which are doubled due to the flipping process, lead to a gain reduction penalty in spectral efficiency.

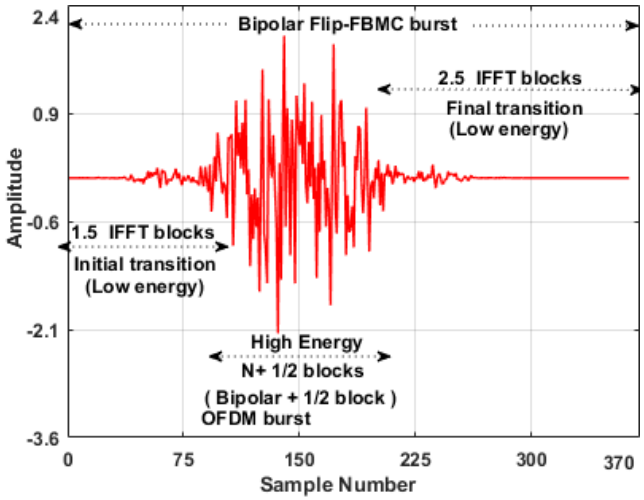

FIGURE 5. Bipolar FBMC burst of a short packet (1 conveyed symbol).

Thus, the mechanism of Flip-FBMC with a filter length of $IFFT_{Size}*K+1$ and $K=4$ imposes a penalty of $2*(K+0.5)$ extra symbols to transmit a Flip-OFDM burst with no CP.

The most significant parts of the transitions can be safely truncated since the average energy of these symbols is very small compared to other higher energy of $(N+1/2)$ bipolar FBMC blocks [30]. Therefore, a hard truncation of the lowest energy tails (1.5 and 2.5 IFFT blocks) over a long burst of data is considered to improve spectral efficiency. It is worth mentioning that with such shortening values, there is a penalty of at least an extra half-symbol, which is doubled to one IFFT block more than the Flip-OFDM burst. However, most redundancy tails can be cut with minor consequences [16]. Hence, the resulting truncation shows a noteworthy influence on the quality of the retrieved signal, as shown in Fig. 6.

To keep the performance of the proposed system identical to that of a Flip-OFDM and by using a Monte Carlo algorithm, different truncations of the redundancy tail have been tested to obtain the optimum shortening values at both ends of the burst.

As observed in Fig. 7, novel truncation values are obtained by leaving part of the redundancy tail at the beginning and end of a bipolar-FBMC packet, which significantly limits the interference level [30]. Thus, $1.5*IFFT_{Size}$ (1.5 symbols) at the initial transition and $1.75*IFFT_{Size}$ (1.75 symbols) at the end of the data burst are discarded. Moreover, Fig. 7 depicts the distributed energy for the truncated tail at both ends of a data packet, where the burst with a Martin filter reduces the energy of a data block further than the IOTA. Note that the assumed truncated values are only valid with an even overlapping factor ($K=4$) and a filter length of $IFFT_{Size}*K+1$. Therefore, the resulting length of a FLIP-FBMC burst in samples can be determined as follows:

$$Truncated\ burst_{(\text{even}K)} = 2^* \left(IFFT_{\text{Size}}{}^* (N + K - 2.75)\right) \tag{19}$$

The subframes ($X^+(k)$ and $X^-(k)$) of the Flip-FBMC signal, as depicted in Fig. 8(a), impose a penalty of 2^* (4) extra IFFT blocks and 2^* (0.5) blocks of an inherent tail. These 9 blocks of symbols (penalty) are minimized as in (19) to only 2.5 extra symbols more than the Flip-OFDM, as observed in Fig. 8(b).

The truncation burst using a Martin filter causes a remarkable degradation in system performance over a long data burst (100 symbols) and high modulation orders (≥64-QAM), while it exhibits an SER performance identical to that of the Flip-OFDM technique over lower mapping, as depicted in Fig. 9. To analyze the performance degradation of the proposed design, the characteristics of the Martin filter have been evaluated in terms of their figures of merit, which are presented in [17]. The Martin filter shows a solid performance for various figures of merit, such as a high quality of the reconstructed signal, reliable signal-to-interference ratio and low OOBE, as presented in Fig. 10. To a certain extent, a low ξ factor is remarkable in the performance of the Martin filter. Furthermore, it is also observed that this factor is improved by deploying a filter with low time and frequency spreading [17], [18]. From that perspective, the IOTA filter in [17] with a near-optimum value of ξ is considered for sake of comparison. The exact ξ of the corresponding work using Martin and IOTA filters of length $IFFT_{Size}*K+1$ can be measured as follows [17], [18], [36]:

$$\xi = 1/4\pi\ \Delta W \Delta T \tag{20}$$

where

$$0 \leq \xi \leq 1 \tag{21}$$

The localization factor ξ is determined by the dispersion product of ΔW and ΔT, where the synthesis filters $g_m(k)$ have the same frequency dispersion (ΔW) and time dispersion (ΔT). The dispersion values can be calculated as:

$$\Delta W = \sqrt{\int_{-\infty}^{\infty} f^2 |P(f)|^2 df} \tag{22}$$

and

$$\Delta T = \sqrt{\int_{-\infty}^{\infty} t^2 |p(t)|^2 dt} \tag{23}$$

where the $p(t)$ term is the prototype pulse function and $p(f)$ is its Fourier transform. Note that employing a filter with ξ close to 1 results in optimum time-frequency pulse localization [18], [36]. As illustrated in Fig. 7, an IOTA filter having a 0.977 localization factor (close to 1) results in concentrating the signal energy according to an envelope function around its center, which leads to lower energy loss than that of a Martin filter having $\xi = 0.8839$ due to hard truncation of the redundancy tails. Consequently, a truncated packet using an IOTA filter exhibits an identical SER performance to that of the Flip-OFDM technique and a superior performance over the shortening burst using a Martin filter with high constellation mapping in a flat VLC channel, as observed in Fig. 9.

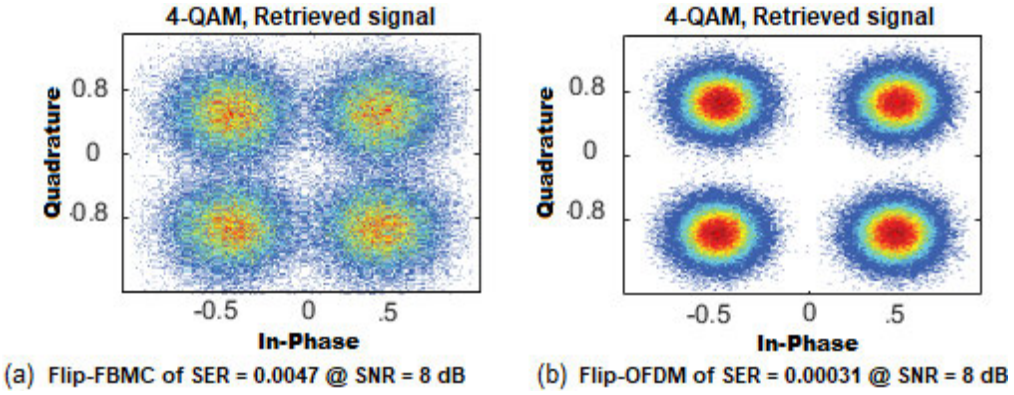

FIGURE 6. Constellations of 4-QAM retrieved signals over a long data burst (100 transmitted symbols) to show (a) the degradation of the Flip-FBMC performance through a hard truncation of the lowest energy parts (1.5 symbols at the beginning of the packet and 2.5 symbols at the end of the data burst) of the tail compared with the classic Flip-OFDM in (b).

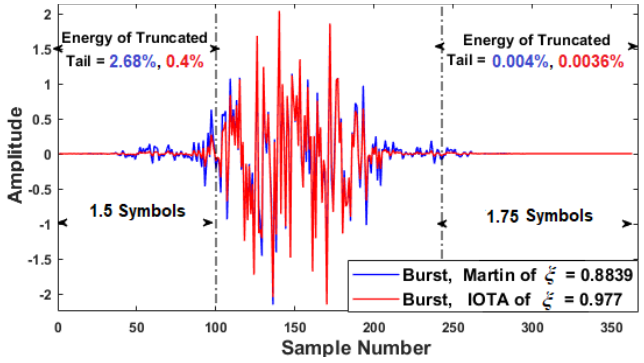

FIGURE 7. Optimal shortening values for the hard truncation method of 1.5 and 1.75 symbols at both ends of a short bipolar burst.

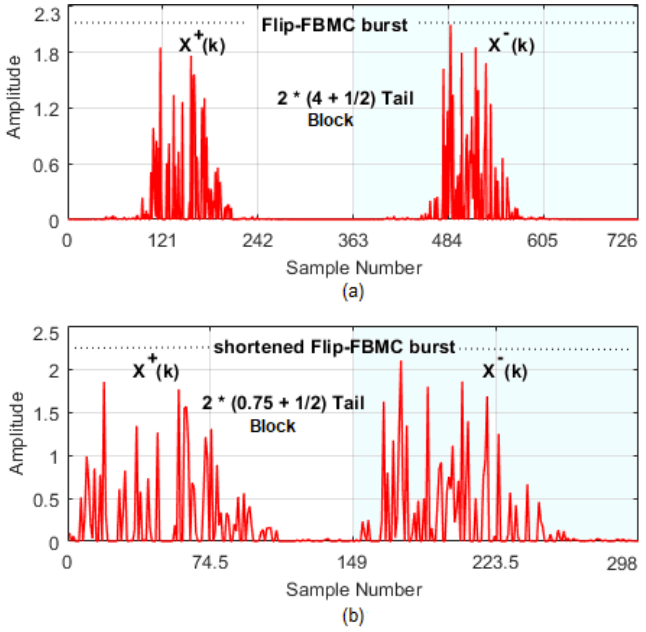

FIGURE 8. Consecutive subframes of a Flip-FBMC burst for (a), and (b) the truncated version of a Flip-FBMC packet.

Moreover, it contributes to reduce the TMUX-latency that presented in (9) as:

$$\Delta\Upsilon_{\text{new}} = \frac{2}{IFFT_{\text{Size}}}\left(L_p - 1 - 1.5\,IFFT_{\text{Size}} + \Delta\delta\right) \qquad (24)$$

where the $1.5^{*}IFFT_{Size}$ term is derived and added to satisfy the shortening of the data packet transmission. Thus, the reconstructed delay is reduced from *2K* to *2K-3* at the AFB output. The truncation effect on the information rate can be observed in Fig. 10, where the throughputs of Flip-FBMC are highly dependent on the packet size (data blocks), and the gain in spectral efficiency is significantly improved at low numbers of IFFT blocks.

V. ANALYSIS PERFORMANCE OF CHANNEL ESTIMATION

As described above, the optical FBMC has drawn wide attention because of its low out-of-band radiation arising from the time-frequency localization of filter banks and the high information rate that results from eliminating CPs and guard bands [37]. The performances of nontruncated and truncated Flip FBMC are evaluated with respect to the traditional one at the LOS channel gain that obtained in section III. In Flip-OFDM, a CP of 1 point length is added to combat ISI, and a one-tap zero forcing (ZF) equalizer-based training block of complex signal duration is used for CE, as detailed in Table 3.

It can be seen from Fig. 11 that the CE of a Flip-FBMC deploys the two variants of IAM (IAM-R and IAM-C) and inserts them in the preamble to suppress the IMI effect. The length of three known sequential pilots is equal to 1.5 training blocks (0.5 blocks more overhead than Flip-OFDM) designed by inserting 2 blocks of zeros in the neighborhood of the maximum pilot power.

The 1st zero-block $P_{m0,n0\text{-}1}$ is employed to prevent interference from the previous frame and the two successive subframes at the flipping stage. The nonzero part of the transmitted pilots $P_{m0,n0}$ is set to the maximum value as presented in Fig. 11, while the 3rd block $P_{m0,n0+1}$ avoids

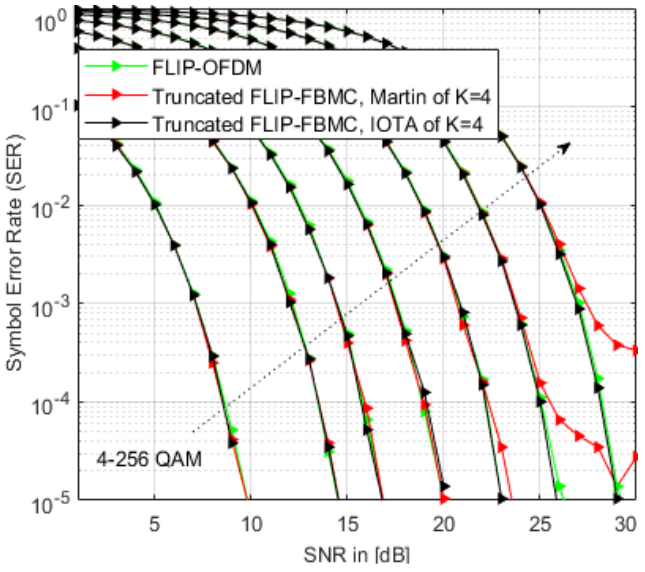

FIGURE 9. Symbol error rate vs SNR over a long data burst for Flip-OFDM and Flip-FBMC employing IOTA and Martin filters of the proposed truncation values of 1.5, and 1.75 symbols at both ends of a bipolar burst in a flat VLC channel.

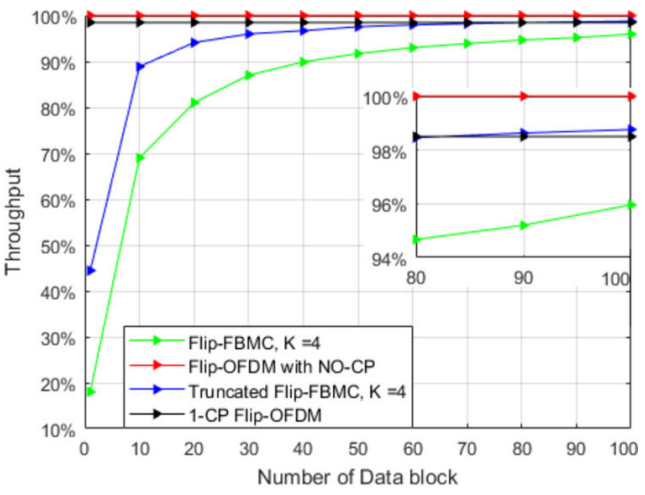

FIGURE 10. Hard truncation impact on spectral efficiency.

interference from the payload data. The received preamble pilots ($PLT_{m0,n0}$) can be calculated as in [11], [27]:

$$PLT_{m0,n0}^{\text{received}} = H_m \left(P_{m0,n0} + jP_{m0,n0}^{\text{imaginary interference}} \right) + Z_{m0,n0} \tag{25}$$

We have considered $N=80$ assuming a subframe of a VLC system. This assumption drives to an overhead of 1.55% residual tail and almost identical throughput to CP of one sample for Flip-OFDM, whereas it creates approximately 5.7% blocks of overhead for a nontruncated packet, as observed in Fig. 10. Further attention is required to obtain a high data bit rate in real-time transmission, as the 3 dB modulation bandwidth of commercially available LEDs is only

TABLE 3. The system parameters for channel estimation.

Parameters	Value	
Utilized technique	Flip FBMC	Flip OFDM
IFFT size	64 samples	
Pilot duration in symbols	1.5	1
Constellation mapping	4-QAM	
Prototype filter	IOTA	Rectangular
Channel tap gain	1-Direct LOS	
CP size	0	1
Overlapping factor (K)	4	Non
Equalization size	1-Tap based CE of IAM-R/C	1-Tap
Number of Transmitted symbols	80 symbols	

several MHz [38]. The limited modulation bandwidth can be extended by using pre- and postequalization techniques [39].

The CE-based IAM for a Flip-FBMC VLC system can be computed as:

$$H_{m,n}^{\wedge} = \frac{PLT_{m0,n0}}{P_{m0,n0} + jP_{m0,n0}^{\text{imaginary interference}}} \tag{26}$$

The $jP_{m0,n0}$ term represents the interference weight, which can be calculated in advance and saved at the receiver with the aid of the interference coefficients FBMC law in [11]. In addition, by using a Monte Carlo algorithm with respect to a traditional Flip-OFDM, the error performance of each nontruncated and truncated Flip-FBMC technique has been evaluated by using CE based on IAM-R and IAM-C. A one-tap ZF equalizer is employed to nullify the LOS channel effect at the output of the

AFB, which can be calculated according to [9], [31].

$$A_{m,n}^{\text{estimated}} = \text{Re}\left\{ \left(\underbrace{\left\langle Y(k), f_{m,n}(k) \right\rangle \downarrow_{\frac{M}{2}}}_{\text{AFB\_output}} H_{m,n}^{\wedge -1} \right) \underbrace{e^{-j\frac{\pi}{2}(m+n)}}_{\varphi_{m,n}*} \right\} \tag{27}$$

Fig. 12 shows the nonshortened/truncated proposed designs' SER with IOTA filters of $K=4$, which are shown for comparison with Flip-OFDM signals using 4-QAM modulation. The truncated Flip-FBMC-based IAM-C exhibits a superior error performance of 1.5 dB at SER= 10^{-3}, which decreases with increasing SNR values to reach 1 dB at 10^{-3} SER compared with the traditional technique. However, the difference between the IAM-R performance and that of IAM-C is due to the required pseudo-pilots in the IAM-C method, which have a larger magnitude than those in IAM-R and hence effectively mitigate the impact of the added Gaussian noise and IMI. Thus, the CE accuracy is further improved. On the other hand, the analysis exposes that the preamble pilots-based IAM-C is slightly impacted by the hard truncation of a transmitted burst in contrast to the

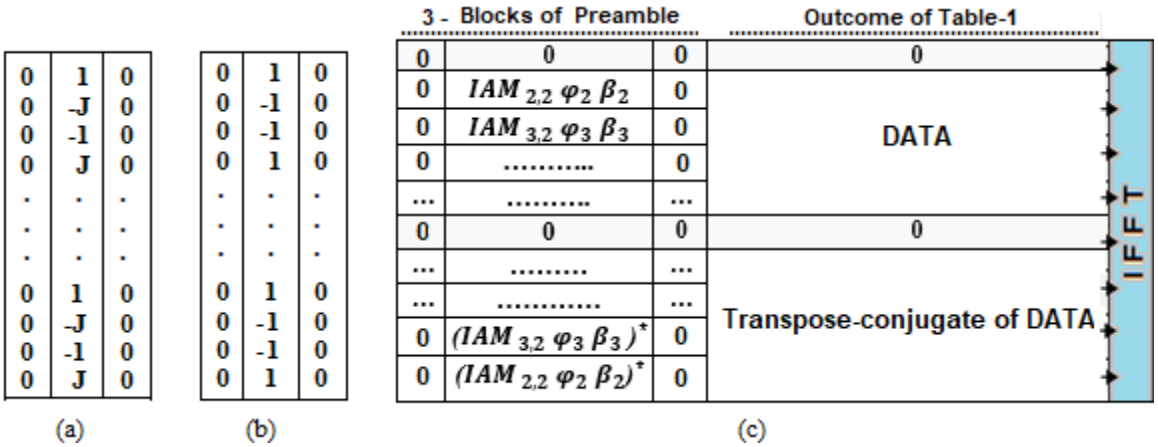

FIGURE 11. Preamble structures for the (a) IAM-C and (b) IAM-R methods and (c) the frame configuration for an FBMC-TMUX VLC system.

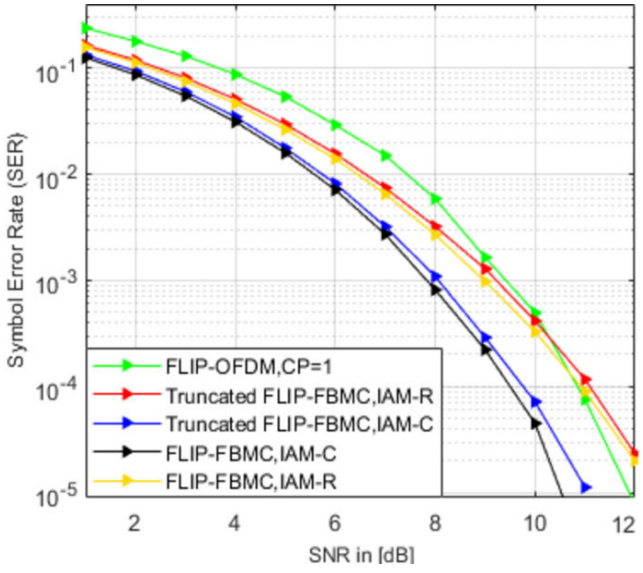

FIGURE 12. SER comparison between the truncated Flip-FBMC scheme and Flip-FBMC using CE-based IAM-R/IAM-C compared with Flip-OFDM of 1-CP in LOS VLC-channel.

nontruncated version [15], while a shortened version using CE-based IAM-R exhibits an almost-identical SER performance to a nontruncated version using IAM-R because the lower magnitude of pseudo-pilots is related to the magnitude of IAM-C reference symbols. It is worth mentioning that the Heisenberg factor application to shortening tails has not been demonstrated before.

In future work, we will study the non-LOS propagation of different multipath scenarios to analyze the expected degradation of a one-tap equalizer, and an efficient multitap equalizer will be investigated to improve the system robustness over a larger delay spread. Additionally, the complex-valued symbol-based FBMC/OQAM (C-FBMC/OQAM) model in [40] is planned to be proposed in IM/DD communication systems since C-FBMC/OQAM represents a key solution to imaginary interference cancellation, having demonstrated better performance than conventional FBMC/OQAM systems through frequency-selective fading channels in an RF field.

To support fifth-generation (5G) application requirements based on optical FBMC, the proposed system can be efficiently deployed to indoor VLC, free space link-based LD and IM/DD passive optical network (PON) systems to enhance system performance [27], [41]. It is worth mentioning that such a low latency is a crucial feature in the Tactile Internet (the next evolution of the Internet of Things) [42].

Although Flip-FBMC has a lower PAPR than DCO-FBMC in [9] due to the DC bias voltage required to obtain the unipolar form, it is worth mentioning that the proposed scheme has a higher PAPR than Flip-OFDM due to the deterministic sequences of IAM preambles [43]. However, this design model can be updated to efficiently reduce the PAPR, as presented in [44].

VI. CONCLUSION

In this work, for the first time to the best of the authors' knowledge, we introduce a Flip-FBMC scheme as a good alternative technique to traditional Flip-OFDM in VLC systems. The proposed scheme is based on a biorthogonal form to provide sufficient flexibility for system design requirements. Moreover, the spectral efficiency is increased by employing a hard truncation method for the redundancy tail with 1.5 symbols of the initial transition and 1.75 symbols of the final transition at both ends of a data burst by using an optimum overlapping factor of 4 and a filter length of $IFFT_{Size} * K+1$. Hence, the penalty for the proposed design is reduced from $2*(K+5)$ to $2*(K-2.75)$ symbols, and the resulting penalty is lower than the DCO-FBMC penalty by 2 IFFT blocks. The impact of tail shortening is evaluated over a long data burst by using IOTA and Martin filters, and as expected from the low time and frequency spreading of the IOTA filter compared to the Martin filter, the results show

concentrated signal energy in an envelope function around its center, which leads to lower energy loss due to the redundancy of a truncated tail. Thus, employing a filter with a Heisenberg factor close to one is considered one of the essential requirements in a tail shortening application. Hence, an identical SER performance is obtained for Flip-FBMC by using an IOTA filter in the traditional Flip-OFDM, while significant degradation is reported for high-modulation mapping with a Martin filter when the optical channel state information is known at the receiver. Moreover, the truncated scheme contributes a reduction of the TMUX latency from *2K* to *2K-3* at the AFB output. The simulation results for LOS channel gain show that a truncated Flip-FBMC-based IAM-C CE displays a superior performance of approximately 1.5 dB at a 10^{-3} SER, which decreases with increasing SNR values to reach 1 dB at 10^{-5} SER over the traditional Flip-OFDM of 1 CP. The degradation in the accuracy of the retrieved signal using an IAM-R preamble is addressed since the magnitudes of the pseudo-pilots are lower than those in IAM-R. On the other hand, the analysis reveals that a preamble pilots-based IAM-C is slightly impacted by hard truncation in contrast to a nontruncated model, while a shortened version using the CE-based IAM-R exhibits almost-identical SER performance to a nontruncated version using IAM-R due to the lower magnitude of IAM-R pseudo-pilots relative to the magnitude of IAM-C reference symbols.

REFERENCES

[1] D. C. O'Brien, L. Zeng, H. Le-Minh, G. Faulkner, J. W. Walewski, and S. Randel, "Visible light communications: Challenges and possibilities," in *Proc. IEEE 19th Int. Symp. Pers., Indoor Mobile Radio Commun.*, Sep. 2008, pp. 1–5.

[2] S. D. Dissanayake and J. Armstrong, "Comparison of ACO-OFDM, DCO-OFDM and ADO-OFDM in IM/DD systems," *J. Lightw. Technol.*, vol. 31, no. 7, pp. 1063–1072, Apr. 1, 2013.

[3] N. Fernando, Y. Hong, and E. Viterbo, "Flip-OFDM for unipolar communication systems," *IEEE Trans. Commun.*, vol. 60, no. 12, pp. 3726–3733, Dec. 2012.

[4] J. Armstrong and B. Schmidt, "Comparison of asymmetrically clipped optical OFDM and DC-biased optical OFDM in AWGN," *IEEE Commun. Lett.*, vol. 12, no. 5, pp. 343–345, May 2008.

[5] R. Islam, P. Choudhury, and M. A. Islam, "Analysis of DCO-OFDM and flip-OFDM for IM/DD optical-wireless system," in *Proc. 8th Int. Conf. Electr. Comput. Eng.*, Dec. 2014, pp. 32–35.

[6] N. Fernando, Y. Hong, and E. Viterbo, "Flip-OFDM for optical wireless communications," in *Proc. IEEE Inf. Theory Workshop*, Oct. 2011, pp. 5–9.

[7] Q. He and A. Schmeink, "Comparison and evaluation between FBMC and OFDM systems," in *Proc. WSA 19th Int. ITG Workshop Smart Antennas*, Ilmenau, Germany, 2015, pp. 1–7.

[8] M. Bellanger, "FBMC physical layer: A primer," ICT-PHYDYAS, Tech. Rep., 2010, pp. 1–31. [Online]. Available: http://www.ict phydyas.org/teamspace/internal-folder/FBMC-Primer_06-2010.pdf

[9] B. Lin, X. Tang, Z. Ghassemlooy, X. Fang, C. Lin, Y. Li, and S. Zhang, "Experimental demonstration of OFDM/OQAM transmission for visible light communications," *IEEE Photon. J.*, vol. 8, no. 5, pp. 1–10, Oct. 2016.

[10] C. Lele, P. Siohan, and R. Legouable, "2 dB better than CP-OFDM with OFDM/OQAM for preamble-based channel estimation," in *Proc. IEEE Int. Conf. Commun.*, May 2008, pp. 1302–1306.

[11] E. Kofidis, D. Katselis, A. Rontogiannis, and S. Theodoridis, "Preamble-based channel estimation in OFDM/OQAM systems: A review," *Signal Process.*, vol. 93, no. 7, pp. 2038–2054, 2013.

[12] M. A. AboulDahab, M. M. Fouad, and R. A. Roshdy, "A proposed preamble based channel estimation method for FBMC in 5G wireless channels," in *Proc. 35th Nat. Radio Sci. Conf. (NRSC)*, Mar. 2018, pp. 140–148.

[13] K. A. Alaghbari, H.-S. Lim, and T. Eltaif, "An improved least squares channel estimation algorithm for coherent optical FBMC/OQAM system," *Opt. Commun.*, vol. 439, pp. 141–147, May 2019, doi: 10.1016/j.optcom.2019.01.012.

[14] X. Fang, Y. Wang, Z. Suo, H. Jiang, X. Gao, L. Zhang, and D. Ding, "Analysis of the time-frequency localization property of the filter banks for optical OFDM/OQAM systems," *J. Lightw. Technol.*, vol. 37, no. 21, pp. 5392–5405, Nov. 1, 2019.

[15] R. Chen, K.-H. Park, C. Shen, T. K. Ng, B. S. Ooi, and M.-S. Alouini, "Visible light communication using DC-biased optical filter bank multi-carrier modulation," in *Proc. IEEE Global LIFI Congr.*, Mar. 2018, pp. 1–6.

[16] M. Bellanger, "Efficiency of filter bank multicarrier techniques in burst radio transmission," in *Proc. IEEE Global Telecommun. Conf. (GLOBECOM)*, Dec. 2010, pp. 1–4.

[17] R. T. Kobayashi and T. Abrao, "FBMC prototype filter design via convex optimization," *IEEE Trans. Veh. Technol.*, vol. 68, no. 1, pp. 393–404, Jan. 2019.

[18] C. Boyd, R.-A. Pitaval, O. Tirkkonen, and R. Wichman, "On the time-frequency localisation of 5G candidate waveforms," in *Proc. IEEE 16th Int. Workshop Signal Process. Adv. Wireless Commun. (SPAWC)*, Jun. 2015, pp. 101–105.

[19] L. G. Baltar, I. Slim, and J. A. Nossek, "Efficient filter bank multicarrier realizations for 5G," in *Proc. IEEE Int. Symp. Circuits Syst. (ISCAS)*, May 2015, pp. 2608–2611.

[20] P. P. Vaidyanathan, *Multirate Systems and Filter Banks*. Englewood Cliffs, NJ, USA: Prentice-Hall, 1993.

[21] P. Siohan, C. Siclet, and N. Lacaille, "Analysis and design of OFDM/OQAM systems based on filterbank theory," *IEEE Trans. Signal Process.*, vol. 50, no. 5, pp. 1170–1183, May 2002.

[22] (Jan. 2009). *INFSO-ICT-211887 Project PHYDYAS, Deliverable 5.1: Prototype Filter and Structure Optimization* [Online]. Available: http://www.ict-phydyas.org/delivrables/PHYDYAS-D5-1.pdf/view

[23] T. Stitz, T. Ihalainen, A. Viholainen, and M. Renfors, "Pilot-based synchronization and equalization in filter bank multicarrier communications," *EURASIP J. Adv. Signal Process.*, vol. 2010, no. 1, pp. 1–18, Dec. 2010.

[24] M. Aldababseh and A. Jamoos, "Estimation of FBMC/OQAM fading channels using dual Kalman filters," *Sci. World J.*, vol. 2014, pp. 1–9, Feb. 2014, doi: 10.1155/2014/586403.

[25] N. van der Neut, B. T. Maharaj, F. de Lange, G. J. González, F. Gregorio, and J. Cousseau, "PAPR reduction in FBMC using an ACE-based linear programming optimization," *EURASIP J. Adv. Signal Process.*, vol. 2014, no. 1, pp. 1–21, Dec. 2014, doi: 10.1186/1687-6180-2014-172.

[26] A. Viholainen, T. Ihalainen, T. H. Stitz, M. Renfors, and M. Bellanger, "Prototype filter design for filter bank based multicarrier transmission," in *Proc. 17th Eur. Signal Process. Conf.*, Aug. 2009, pp. 1359–1363.

[27] J. Shi, J. He, R. Zhang, and R. Deng, "Experimental demonstration of blind equalization for OFDM/OQAM-VLC system," *Opt. Eng.*, vol. 58, no. 6, p. 1, Jun. 2019.

[28] C.-W. Chen and F. Maehara, "An enhanced MMSE subchannel decision feedback equalizer with ICI suppression for FBMC/OQAM systems," in *Proc. Int. Conf. Comput., Netw. Commun. (ICNC)*, Jan. 2017, pp. 1041–1045.

[29] T. Komine and M. Nakagawa, "Fundamental analysis for visible-light communication system using LED lights," *IEEE Trans. Consum. Electron.*, vol. 50, no. 1, pp. 100–107, Feb. 2004.

[30] M. Ijaz, D. Tsonev, A. Stavridis, A. Younis, J. J. D. McKendry, E. Gu, M. D. Dawson, S. Videv, and H. Haas, "Optical spatial modulation OFDM using micro LEDs," in *Proc. 48th Asilomar Conf. Signals, Syst. Comput.*, Nov. 2014, pp. 1734–1738.

[31] D. W. M. Guerra and T. Abrão, "Efficient multitap equalization for FBMC-OQAM systems," *Trans. Emerg. Telecommun. Technol.*, vol. 30, no. 12, Dec. 2019, Art. no. e3775, doi: 10.1002/ett.3775.

[32] A. Zafar, M. A. Imran, P. Xiao, A. Cao, and Y. Gao, "Performance evaluation and comparison of different multicarier modulation schemes," in *Proc. IEEE 20th Int. Workshop Comput. Aided Modeling Design Commun. Links Netw. (CAMAD)*, Sep. 2015, pp. 49–53.

[33] Z. He, L. Zhou, Y. Chen, and X. Ling, "Filter optimization of out-of-band emission and BER analysis for FBMC-OQAM system in 5G," in *Proc. IEEE 9th Int. Conf. Commun. Softw. Netw. (ICCSN)*, May 2017, pp. 56–60.

[34] S. Taheri, M. Ghoraishi, P. Xiao, and L. Zhang, "Efficient implementation of filter bank multicarrier systems using circular fast convolution," *IEEE Access*, vol. 5, pp. 2855–2869, 2017.

[35] A.-A. Husam and Z. Kollar, "Complexity comparison of filter bank multicarrier transmitter schemes," in *Proc. 11th Int. Symp. Commun. Syst., Netw. Digit. Signal Process. (CSNDSP)*, Jul. 2018, pp. 1–4.
[36] R. Haas and J.-C. Belfiore, "Multiple carrier transmission with time-frequency well-localized impulses," in *Proc. IEEE 2nd Symp. Commun. Veh. Technol.*, Brussels, Belgium: Benelux, Nov. 1994, pp. 187–193.
[37] Y. Fu, X. Fang, X. Sui, L. Zhang, D. Ding, and X. Gao, "Analysis of the pseudo pilot in optical OFDM/OQAM system," in *Proc. 12th Int. Conf. Commun. Softw. Netw. (ICCSN)*, Jun. 2020, pp. 161–165.
[38] D. H. Kwon, S. H. Yang, and S. K. Han, "Modulation bandwidth enhancement of white-LED-based visible light communications using electrical equalizations," *Proc. SPIE*, vol. 9387, Feb. 2015, Art. no. 93870T, doi: 10.1117/12.2078680.
[39] N. Fujimoto and H. Mochizuki, "477 Mbit/s visible light transmission based on OOK-NRZ modulation using a single commercially available visible LED and a practical LED driver with a pre-emphasis circuit," in *Proc. Opt. Fiber Commun. Conf./Nat. Fiber Optic Eng. Conf.*, Mar. 2013, pp. 1–3.
[40] D. Kong, X. Zheng, Y. Zhang, and T. Jiang, "Frame repetition: A solution to imaginary interference cancellation in FBMC/OQAM systems," *IEEE Trans. Signal Process.*, vol. 68, pp. 1259–1273, 2020.
[41] M. F. Sanya, L. Djogbe, A. Vianou, and C. Aupetit-Berthelemot, "DC-biased optical OFDM for IM/DD passive optical network systems," *J. Opt. Commun. Netw.*, vol. 7, no. 4, pp. 205–214, Apr. 2015.
[42] S. K. Sharma, I. Woungang, A. Anpalagan, and S. Chatzinotas, "Toward tactile internet in beyond 5G era: Recent advances, current issues, and future directions," *IEEE Access*, vol. 8, pp. 56948–56991, 2020.
[43] D. Kong, J. Li, K. Luo, and T. Jiang, "Reducing pilot overhead: Channel estimation with symbol repetition in MIMO-FBMC systems," *IEEE Trans. Commun.*, vol. 68, no. 12, pp. 7634–7646, Dec. 2020.
[44] D. Kong, X. Zheng, Y. Yang, Y. Zhang, and T. Jiang, "A novel DFT-based scheme for PAPR reduction in FBMC/OQAM systems," *IEEE Wireless Commun. Lett.*, vol. 10, no. 1, pp. 161–165, Jan. 2021.

MOHAMMED S. BAHAAELDEN received the B.Sc. degree in electronic engineering from Mosul University, Iraq, 2008, the M.Sc. degree in electrical and electronic engineering from Near East University, North Cyprus, in 2015, and the master's degree in engineering physics from Sofia University, Bulgaria, in 2017. He is currently pursuing the Ph.D. degree in telecommunication engineering with the Polytechnic University of Valencia, Spain, with a focus on optical and quantum communications. His current research interests include future optical wireless communications, 5G-optical FBMC modulation, free-space optical communication, and indoor communication.

BEATRIZ ORTEGA (Member, IEEE) received the M.Sc. degree in physics from the Universidad de Valencia, in 1995, and the Ph.D. degree in telecommunications engineering from the Universitat Politécnica de València, in 1999. She currently works with the Departamento de Comunicaciones, Universitat Politècnica de València, where she also holds a full professorship, since 2009, and collaborates as a Group Leader with the Photonics Research Labs, Institute of Telecommunications and Multimedia Applications. She is also a Co-Founder of Ephoox company. She has participated in a large number of European Networks of Excellence and Research and Development projects and other national ones. She has published more than 200 articles and conference contributions in fiber Bragg gratings, microwave photonics, and optical networks. She has held several patents. Her main research interests include optical devices, optical networks, and microwave photonic systems and applications.

RAFAEL PÉREZ-JIMÉNEZ received the M.Sc. degree from the Universidad Politécnica de Madrid, in 1991, and the Ph.D. degree in telecommunications engineering from the Universidad de Las Palmas de Gran Canaria, in 1995. He is currently a Director of the IDeTIC University Research Institute. He also holds a full professorship with the Universidad de Las Palmas de Gran Canaria, since 2003. He has published more than 250 publications including books, book chapters, articles, and conferences in the field of the visible light systems for indoor communication and its applications for data transmission and positioning. He has contributed in many European research projects, such as the applications of sensor networks and the Internet of Things at smart cities. His main research interests include the field of visible light communications systems, optical camera communications, and the Internet of Things (IoT) network characterization.

MARKKU RENFORS (Life Fellow, IEEE) received the D.Tech. degree from the Tampere University of Technology (TUT), Tampere, Finland, in 1982. Since 1992, he has been a Professor with the Department of Electronics and Communications Engineering, TUT, where he was the Head, from 1992 to 2010. His research interests include filterbank-based multicarrier systems and signal processing algorithms for flexible communications receivers and transmitters. He was a co-recipient of the Guillemin Cauer Award (together with T. Saramäki) from the IEEE Circuits and Systems Society, in 1987.